Published in IET Microwaves, Antennas & Propagation
Received on 7th August 2013
Revised on 23rd November 2013
Accepted on 9th January 2014
doi: 10.1049/iet-map.2013.0430

ISSN 1751-8725

Array configuration optimisation of dual-band controlled reception pattern antenna arrays for anisotropic ground platforms

Gangil Byun[1], *Hosung Choo*[2], *Sunwoo Kim*[1]

[1]*Department of Electronics and Computer Engineering, Hanyang University, Seoul, Korea*
[2]*School of Electronic and Electrical Engineering, Hongik University, Seoul, Korea*
E-mail: remero@hanyang.ac.kr

Abstract: This study proposes a systematic optimisation process of array configurations for controlled reception pattern antenna arrays. The array consists of a single reference antenna at the centre and four auxiliary antennas at the outer perimeter and is mounted on an anisotropic ground platform with an inter-element spacing of about 0.3λ. Only the mounting angles are adjusted to find the optimum array configuration. The proposed process is evaluated by comparing its performance with the global optimum, a conventional array configuration and random array configurations. The results demonstrate that the proposed process achieves a radiation gain close to the global optimum, and no significant gain reductions are found in the auxiliary antennas.

1 Introduction

Controlled reception pattern antenna (CRPA) arrays are widely adopted in many applications to prevent tracking failure of a Global Positioning System (GPS). These arrays are used to form adaptive pattern nulls to minimise the power of undesired interferences while maximising the power of satellite signals [1–3]. In this CRPA operation, one of the array elements operates as a reference antenna and is primarily used when the power of interferences is much weaker than that of satellite signals. The other array elements function as auxiliary antennas in the presence of interferences and are usually arranged in a uniform circular array with the reference antenna placed at the centre of the array [4]. This array configuration allows the system to sustain reliable signal reception at all times when the inter-element spacing is half of a wavelength [5]. However, the available diameter of the array for most CRPA applications is often limited to only a few centimeters in diameter [6], which generates a strong mutual coupling between the centre reference antenna and the surrounding auxiliary antennas [7–9]. Thus, the performance of the reference antenna is significantly degraded by the coupling effect and turns out to be sensitive to the position and direction of the surrounding antennas [10, 11]. This sensitivity becomes much higher when the shape of a ground platform is anisotropic, that is, the platform is non-radial and asymmetric with respect to the centre of the array, which obstructs finding the optimum array configuration in practice [12].

In this paper, we propose a systematic optimisation process of array configurations for CRPA arrays to maximise the gain of the reference antenna. The array consists of five identical dual-band GPS antenna elements, one of which operates as a reference antenna while the others function as auxiliary antennas. The reference antenna is placed at the centre (Port 1), and the auxiliary antennas are arranged in a uniform circular array at the outer perimeter (Port 2, Port 3, …, Port 5). In our process, an anisotropic ground platform with an inter-element spacing of about 0.3λ is used, which was pre-allocated by the system specifications. To achieve the best performance in the given area, only the mounting angles are adjusted by discrete steps of $\Delta\varphi = 90°$, that is, 0°, 90°, 180° and 270°. Thus, the optimum configuration of the five-element array can be found by comparing 20 cases ($20 = 4 \times 5$), which is more than 500 times smaller than the total number of cases ($1024 = 4^5$). The proposed process is evaluated by comparing its performance with the global optimum, a conventional array configuration [13] and random array configurations. In addition, the antenna characteristics, such as reflection coefficients, radiation patterns and gains, are measured in a full anechoic chamber for further verification. The results confirm that the proposed process achieves a high radiation gain of the reference antenna without significant gain degradations of the auxiliary antennas, while reducing the computational load and time.

2 Array configuration optimisation

2.1 Design of individual antennas

Fig. 1 shows the geometry of an individual antenna element in a five-element CRPA array. The antenna has two radiators of

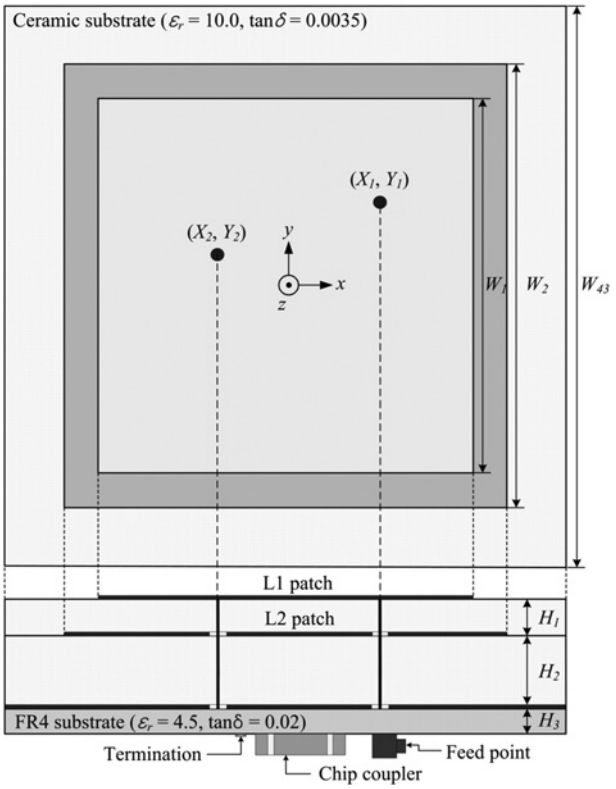

Fig. 1 *Individual antenna structure*

L1 and L2 patches with an RF circuit that contains an external chip coupler (XC1400P-03S, Anaren) and a 50-Ω termination chip [14]. The L1 patch is directly connected to the coupler by two pins and is electromagnetically coupled with the L2 patch. The widths of the patches (W_1 and W_2) are designed to be about a half wavelength in each frequency band, and the coupling strength between the patches is adjusted by the substrate heights (H_1, H_2 and H_3). The feeding positions, (X_1, Y_1) and (X_2, Y_2), are determined by considering both impedance matching and circular polarisation characteristics. To improve the radiation gain and matching characteristics even more, detailed parameters are optimised by using a genetic algorithm [15] in conjunction with the FEKO electromagnetic simulator [16], and the optimised parameters are shown in Table 1. Fig. 2 shows the geometry of an anisotropic ground platform that has the same curvature as a cylindrical vessel whose diameter is 171.5 mm. Fig. 2*a* shows the perspective view of the platform with mounting positions of the antennas, and Fig. 2*b* represents detailed dimensions of the platform and the radome (poly-carbonate with $\varepsilon_r = 2.2$ and tan$\delta = 0.002$).

Table 1 Parameters of the optimised antenna

Parameter	Length, mm
W_1	33.4
W_2	40.0
W_3	50.0
X_1	6.2
X_2	−11.3
Y_1	7.8
Y_2	3.0
H_1	3.14
H_2	7.85
H_3	0.8

In this platform, the inter-element spacing between the reference antenna and each of the surrounding auxiliary antennas is about 0.3λ, which means that the antennas are tightly coupled with the isolation values of about 15 dB.

2.2 Proposed process

Fig. 3 shows a flowchart of the proposed process that optimises the array configuration to maximise the gain of the reference antenna. For this process, the antenna elements are positioned to allow the maximum inter-element spacing in the given area, but the mounting angles (φ_{Port1}, φ_{Port2}, …, φ_{Port5}) of the five antennas are adjusted, as can be seen in Fig. 4. Discrete steps of $\Delta\varphi = 90°$ are chosen for our process to limit the total number of cases to 1024. Each angle is evaluated by the average bore-sight gain of the centre reference antenna in the GPS L1 and L2 bands. The process begins with finding the optimal configuration of the reference antenna. First, we place the reference antenna at the centre of the array and vary its mounting angle (φ_{Port1}) to find the maximum cost by itself. Our cost function, C_{nm} for nth port and mth direction, is defined as an average bore-sight gain at 1.5754 and 1.2276 GHz, and the costs are saved in cost matrix $\bar{\boldsymbol{C}}$. Then, the second antenna is added at port 2, and its optimum mounting angle is determined by considering the bore-sight gain of the reference antenna. The full array configuration with the best performance can be found by repeating this procedure up to port 5. Note that the mounting angles, determined in the previous ports, are fixed until the end of the process. In the entire process, we only observe the average bore-sight gain of the reference antenna to minimise both gain degradation and pattern distortion in the given area, because smaller mutual coupling does not always ensure less pattern distortion. To evaluate the array configuration obtained from the proposed process, the performance of the configuration is compared with that of the global optimum, the conventional array configuration presented in [13], and random array configurations, as shown in Fig. 5. The horizontal axes of the figures represent the number of antennas, for example, only the centre reference antenna exists when the number of antennas is one, and five antennas are fully arranged when the value is five. The global optimum values were achieved by performance evaluations after 1024 ($=4^5$, under the assumption of $\Delta\varphi = 90°$) simulations, thus a total running time of about 1536 h was spent on a computer with an Intel Core i7–3820 quad-core processor and 64 GB of RAM. The performance of the random array configuration was obtained by averaging the results of 20 simulations that were randomly generated. The reason for taking 20 random configurations was because our process requires only 20 iterations for the whole process, which is more than 500 times less computational load compared to the total number of cases. Table 2 shows the mounting angles of these configurations, and Fig. 5*a* shows comparison of gain variations according to the array configurations. The average bore-sight gain of the reference antenna is degraded as the number of antennas increases, which is caused by decreased radiation efficiency because of mismatch loss, as can be seen in Fig 5*b*. However, the proposed configuration consistently maintains a higher radiation gain with lower mismatch loss, which is close to the global optimum. Thus, the bore-sight gain of the five-element array is improved by 1.6 and 1.9 dB compared to the conventional and the random configurations, respectively.

doi: 10.1049/iet-map.2013.0430

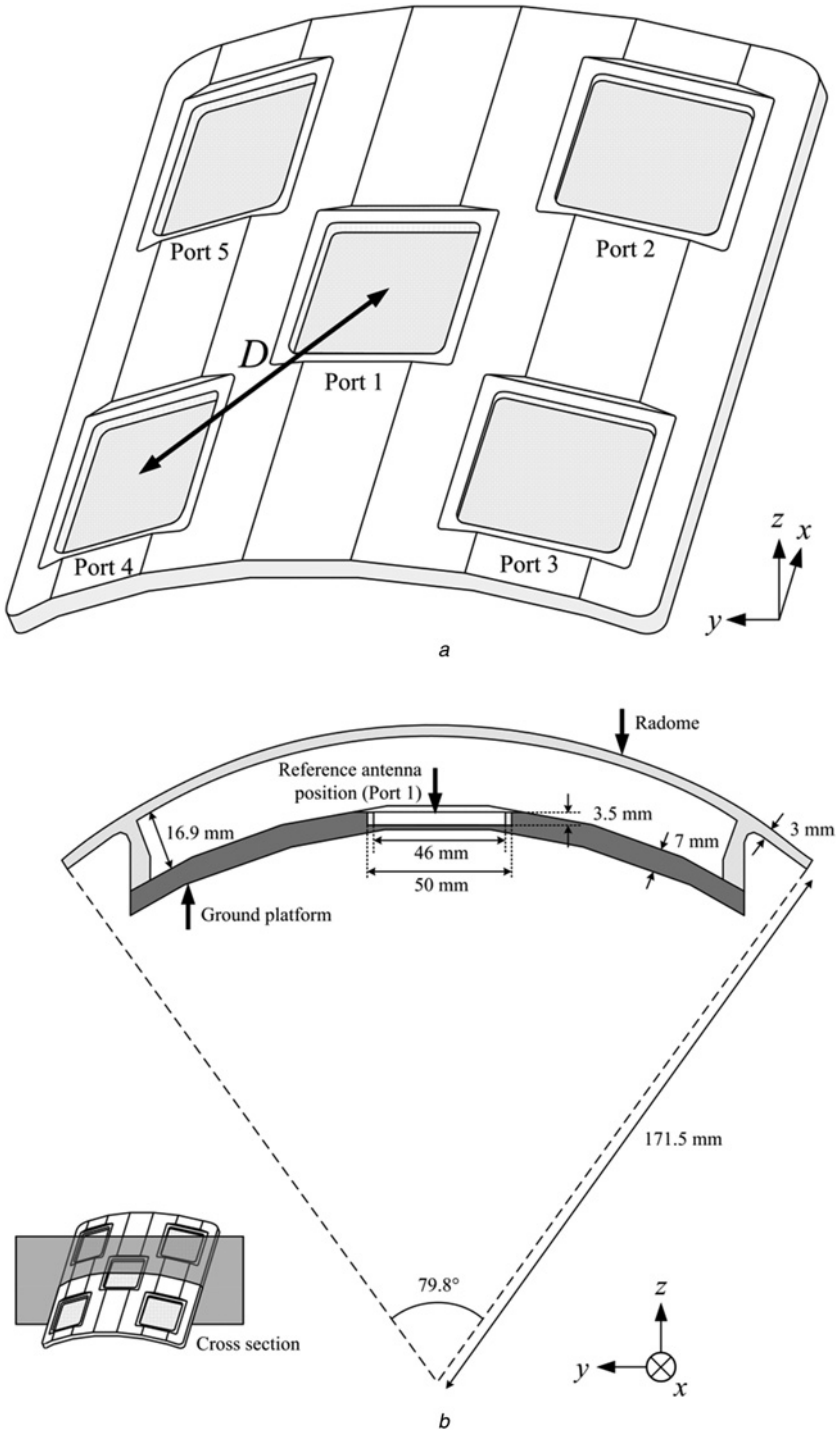

Fig. 2 *Geometry of the ground platform*

a Isotropic view
b Side view

3 Measurement and evaluation

Five antennas were fabricated on a ceramic substrate (CER10, $\varepsilon_r = 10$, $\tan\delta = 0.0035$) obtained from Taconic and then arranged in the proposed configuration on the ground platform that is made of brass ($\sigma = 1.6 \times 10^7$), as shown in Fig. 6, and antenna characteristics, such as the reflection coefficient, radiation gains and patterns, were measured in a full anechoic chamber. Fig. 7*a* and *b* show reflection coefficients and bore-sight gain of the centre reference antenna, respectively. The antenna shows broad matching characteristics with the measured reflection coefficients of −23.8 dB in the GPS L1 band and −19.5 dB in the GPS L2 band. In addition, high radiation gains of 2.0 and −0.1 dBic are achieved in the GPS L1 and L2 bands, respectively. Other measured data, such as reflection coefficients and mutual coupling of the array, are specified in Table 3. Fig. 8 shows the measured radiation patterns in comparison with the simulation. Figs. 8*a* and *b* show patterns in the *zx*- and *zy*-planes, respectively, at 1.5754 GHz, and their

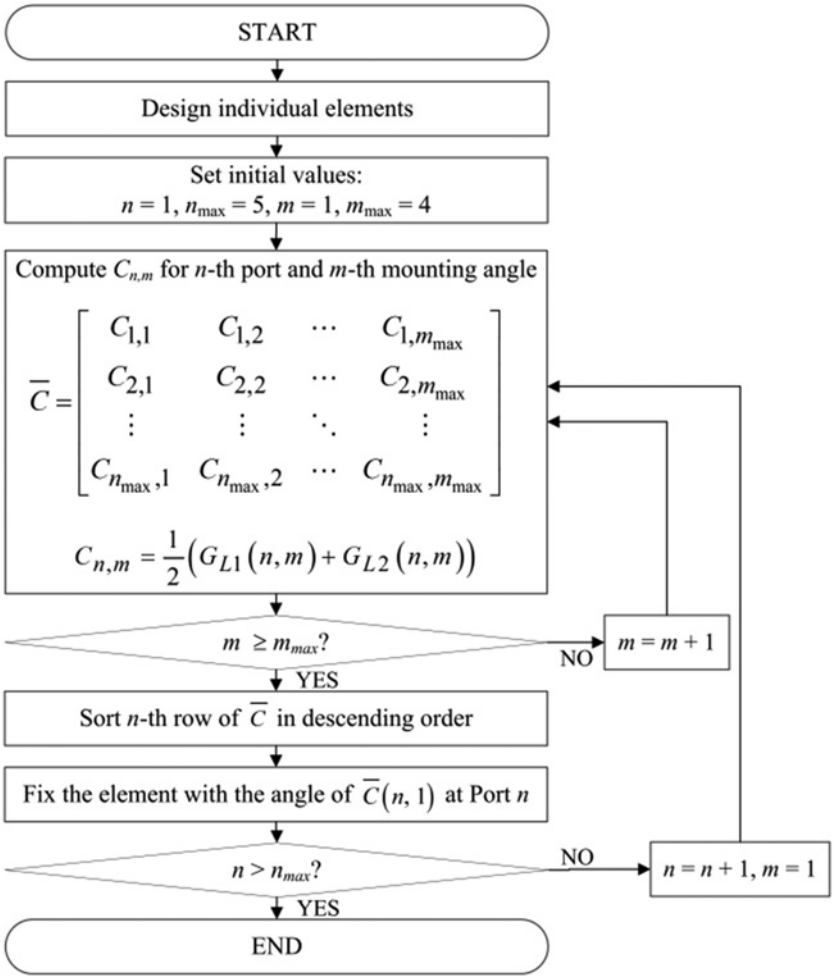

Fig. 3 *Flowchart of the proposed process*

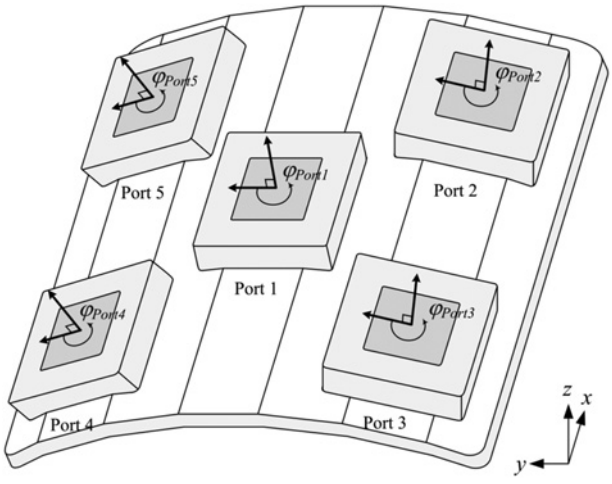

Fig. 4 *CRPA array structure*

half-power beam widths (HPBWs) are 101.2° and 120.7°, respectively. Figs. 8*c* and *d* show the same planes at 1.2276 GHz with HPBWs of 134.1° and 144.7°, respectively. As can be observed, the antenna satisfies the HPBWs of greater than 90° without any serious gain degradation or pattern distortions in both frequency bands. To further verify the suitability of the proposed process, bore-sight gains of auxiliary antennas arranged in the proposed configuration were measured, as shown in Fig. 9, and their average gains are −1.0 dB in the GPS L1 band and −2.5 dB in the GPS L2 band. The average bore-sight gain of the auxiliary antennas is slightly lower than that of the reference antenna because the area of the ground platform around each auxiliary antenna is smaller than the area around the centre antenna, which results in reduced directivity to the bore-sight direction. However, the measured results still demonstrate that the proposed process is capable of improving the gain of the reference antenna without significant gain reductions on auxiliary antennas, which is desired in CRPA arrays. For verification, we calculated a CRPA pattern when a jammer is located at $\varphi = 90°$ and $\theta = 75°$. The optimum weights, applied for each array element to mitigate the effect of the jammer, can be written as (see (1))

$$\bar{W}_{\text{opt}} = \begin{bmatrix} 0.9 & +0.09i & 1.62 & +2.09i & 2.21 & +1.06i & -0.73 & -0.46i & -0.03 & -0.03i \end{bmatrix} \quad (1)$$

which is obtained by the power inversion method [17]. As can be seen, the pattern forms a deep null to the jammer direction with a gain of −45.6 dBi without significant pattern distortions to other directions.

doi: 10.1049/iet-map.2013.0430

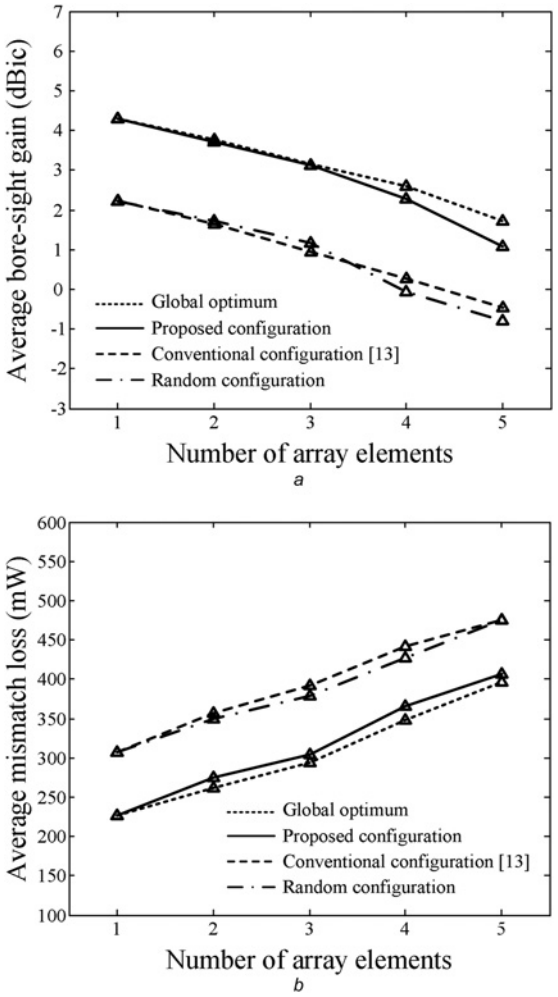

Fig. 5 *Comparison with the random configuration*

a Average bore-sight gain
b Average mismatch loss

Table 2 Mounting angles of various configurations

Configurations	Port 1	Port 2	Port 3	Port 4	Port 5
proposed configuration	270°	90°	180°	270°	0°
global optimum	270°	180°	180°	0°	0°
conventional configuration	0°	90°	180°	270°	0°
	90°	180°	270°	0°	90°
	180°	270°	0°	90°	180°
	270°	0°	90°	180°	270°
random configuration	180°	270°	270°	180°	270°
	180°	90°	90°	270°	270°
	180°	180°	270°	0°	180°
	270°	0°	270°	180°	270°
	0°	180°	90°	270°	90°
	0°	0°	180°	180°	270°
	180°	180°	270°	180°	180°
	180°	0°	270°	270°	270°
	180°	270°	180°	270°	270°
	90°	0°	270°	90°	270°
	90°	270°	270°	180°	180°
	270°	270°	180°	180°	180°
	270°	270°	180°	270°	270°
	270°	180°	90°	270°	90°
	270°	180°	270°	0°	180°
	90°	270°	270°	270°	180°
	270°	180°	90°	180°	0°
	180°	180°	180°	270°	270°
	180°	180°	270°	270°	270°
	270°	180°	90°	270°	90°

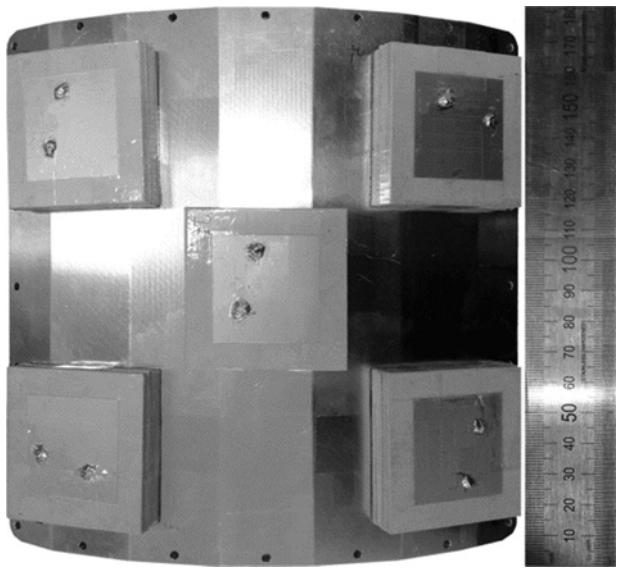

Fig. 6 *Photograph of the fabricated array*

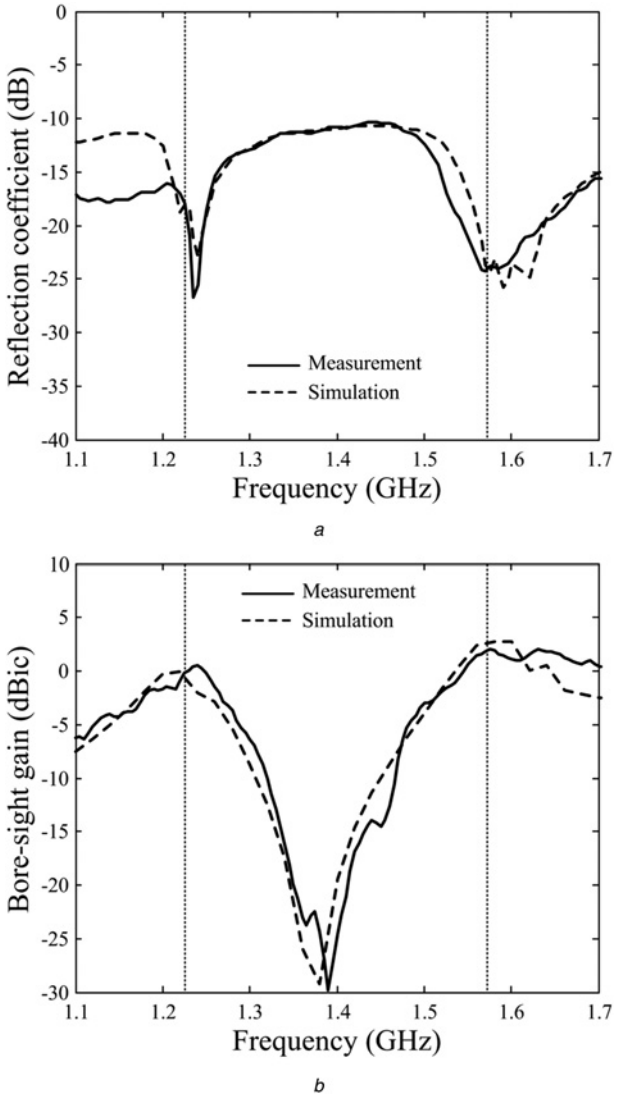

Fig. 7 *Performances of the reference antenna*

a Reflection coefficient
b Bore-sight gain

Table 3 Measured reflection coefficients and mutual coupling

Properties	Frequency	Parameters	Values, dB
reflection coefficients	1.5754 GHz	S_{11}	−23.8
		S_{22}	−23.9
		S_{33}	−10.1
		S_{44}	−12.7
		S_{55}	−17.6
	1.2276 GHz	S_{11}	−19.5
		S_{22}	−19.1
		S_{33}	−10.6
		S_{44}	−16.2
		S_{55}	−8.7
mutual coupling	1575.42 MHz	S_{21}	−23.11
		S_{31}	−23.92
		S_{41}	−23.68
		S_{51}	−19.66
	1.2276 GHz	S_{21}	−21.55
		S_{31}	−19.29
		S_{41}	−27.72
		S_{51}	−19.61

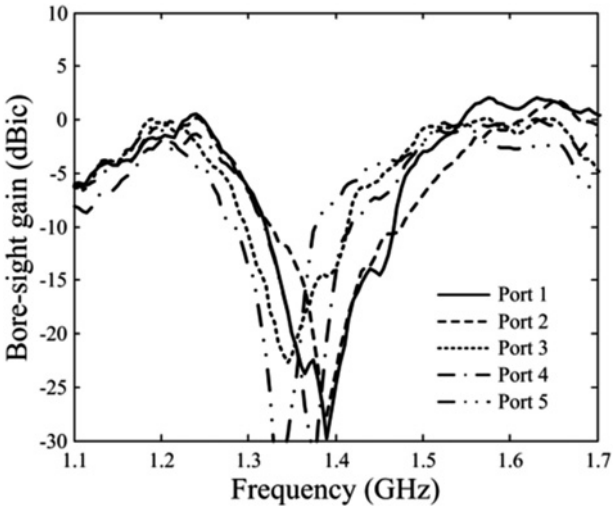

Fig. 9 *Bore-sight gain of CRPA array antennas*

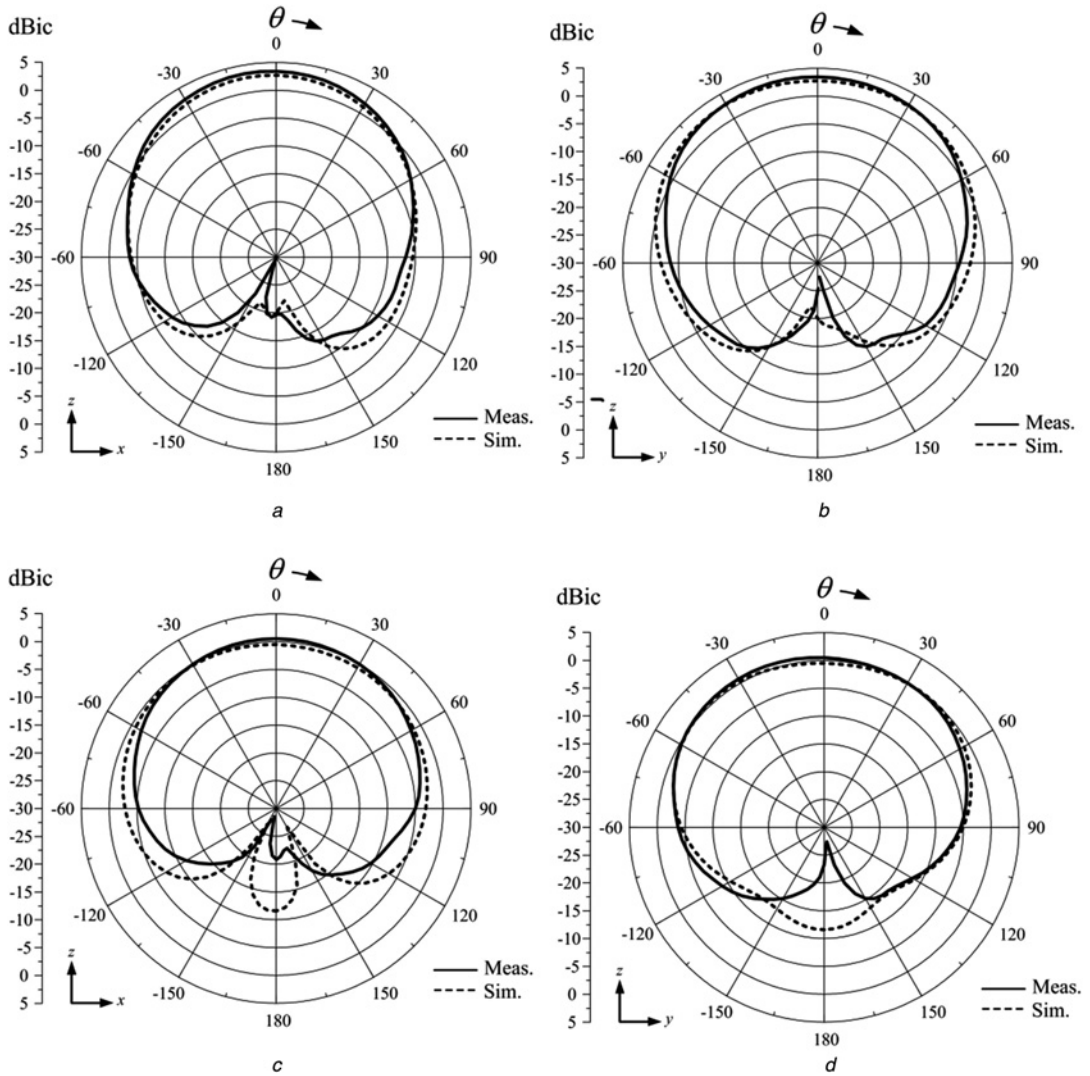

Fig. 8 *Radiation patterns of the reference antenna*

a *zx*-plane at GPS L1 band
b *zy*-plane at GPS L1 band
c *zx*-plane at GPS L2 band
d *zy*-plane at GPS L2 band

doi: 10.1049/iet-map.2013.0430

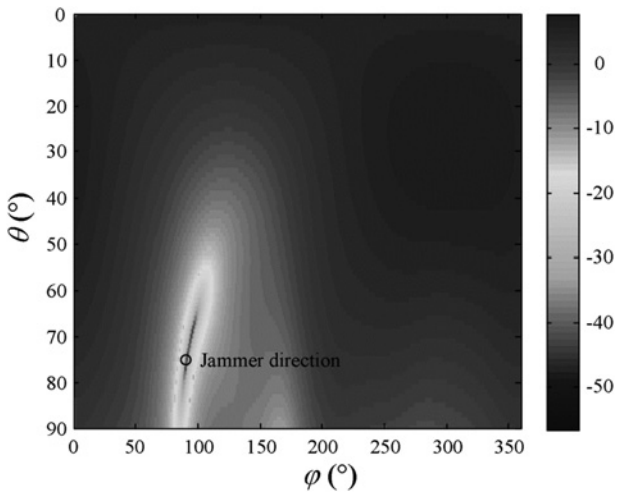

Fig. 10 *Three-dimensional radiation pattern of the CRPA array when a jammer exists at $\varphi = 90°$ and $\theta = 75°$*

4 Conclusion

We investigated the systematic process for optimising the array configuration of a CRPA array to maximise the gain of the reference antenna. The individual antenna was designed to resonate in GPS L1 and L2 bands by using two patches with the external chip coupler. The CRPA array was composed of the single reference antenna at the centre and four auxiliary antennas at the outer perimeter. The array was mounted on the anisotropic ground platform with an inter-element spacing of about 0.3λ. Only the mounting angles were adjusted by the process, and the configuration giving the highest gain for the centre reference antenna was chosen as the proposed array configuration. The suitability of our process was verified by measuring antenna characteristics, such as the reflection coefficient, radiation gains and patterns. In addition, the proposed array configuration obtained by our process was compared to the global optimum, the conventional configuration and random configurations. The results demonstrated that the proposed process achieved the radiation gain close to the global optimum without significant gain degradations of the auxiliary antennas.

5 Acknowledgments

This research was supported by Navcours and the MSIP (Ministry of Science, ICT&Future Planning), Korea, under the ITRC (Information Technology Research Center) support program (NIPA-2013-H0301-13-2007) supervised by the NIPA (National IT Industry Promotion Agency).

6 References

1 Fante, R., Vaccaro, J.J.: 'Wideband cancellation of interference in a GPS receive array', *IEEE Trans. Aerosp. Electron. Syst.*, 2000, **36**, (2), pp. 549–564
2 Zhang, Y.D., Amin, M.G.: 'Array processing for nonstationary interference suppression in DS/SS communications using subspace projection techniques', *IEEE Trans. Signal Process.*, 2001, **49**, (12), pp. 3005–3014
3 Zhang, Y.D., Amin, M.G.: 'Anti-jamming GPS receiver with reduced phase distortions', *IEEE Signal Process. Lett.*, 2012, **19**, (10), pp. 635–638
4 Lambert, J.R., Balanis, C.A., DeCarlo, D.: 'Spherical cap adaptive antennas for GPS', *IEEE Trans. Antennas Propag.*, 2009, **57**, (2), pp. 406–413
5 Balanis, C.A.: 'Antenna theory: analysis and design' (New York, Wiley, 1982, 2005, 3rd edn.)
6 Rabemanantsoa, J., Sharaiha, A.: 'Size reduced multi-band printed quadrifilar helical antenna', *IEEE Trans. Antennas Propag.*, 2011, **59**, (9), pp. 3138–3143
7 Su, T., Ling, H.: 'On the simultaneous modeling of array mutual coupling and array-platform interactions', *Microw. Opt. Technol. Lett.*, 2002, **33**, (3), pp. 167–171
8 Gupta, I.J., Ksienski, A.A.: 'Effect of mutual coupling on the performance of adaptive arrays', *IEEE Trans. Antennas Propag.*, 1983, **AP-31**, (5), pp. 785–791
9 Chen, S.-C., Wang, Y.-S., Chung, S.-J.: 'A decoupling technique for increasing the port isolation between two strongly coupled antennas', *IEEE Trans. Antennas Propag.*, 2008, **56**, (12), pp. 3650–3658
10 Dandekar, K.R., Ling, H., Xu, G.: 'Effect of mutual coupling on direction finding in smart antenna applications', *Electron. Lett.*, 2000, **36**, (22), pp. 1889–1891
11 Su, T., Ling, H.: 'Array beamforming in the presence of a mounting tower using genetic algorithms', *IEEE Trans. Antennas Propag.*, 2005, **53**, (6), pp. 2011–2019
12 Huang, J.: 'The finite ground plane effect on the microstrip antenna radiation patterns', *IEEE Trans. Antennas Propag.*, 1983, **AP-31**, (4), pp. 649–653
13 Huang, J.: 'A technique for an array to generate circular polarization with linearly polarized elements', *IEEE Trans. Antennas Propag.*, 1986, **34**, (9), pp. 1113–1124
14 'XC1400P-03S', http://www.anaren.com, accessed November 2012
15 Rahmat-Samii, Y., Michielssen, E.: 'Electromagnetic optimization by genetic algorithms' (New York, Wiley, 1999, 1st edn.)
16 'FEKO Suite 6.2', http://www.feko.info, accessed November 2012
17 Compton, R.T.Jr.: 'The power-inversion adaptive array: concept and performance', *IEEE Trans. Aerosp. Electron. Syst.*, 1979, **AES-15**, (6), pp. 803–814